Dual Hepatocyte-Targeting Fluorescent Probe with High Sensitivity to Tumorous pH: Precise Detection of Hepatocellular Carcinoma Cells

Yamin Zhang,[a,d] Zhenjie Li,[b] Haibo Ge,[c] Xueyan Zhu,[e] Zhuang Zhao,[e] Zhong-quan Qi,[a] Mian Wang*[b] and Jianyi Wang*[a,d]

[a]*Medical College, Guangxi University, Nanning 530004, China. E-mail: jianyiwang@gxu.edu.cn (W. J.)*

[b]*College of Life Science and Technology, Guangxi University, Nanning 530004, China. E-mail: mianwang@gxu.edu.cn (W. M.)*

[c]*Department of Chemistry and Chemical Biology, Indiana University-Purdue University Indianapolis, Indianapolis, Indiana 46202, USA*

[d]*School of Chemistry and Chemical Engineering, Guangxi University, Nanning 530004, China*

[e]*Guangxi Institute for Food and Drug Control, Nanning 530021, China*

ABSTRACT: A new dual hepatocyte-targeting fluorescent probe **HPL-1**, which can precisely distinguish tumorous pH from physiological pH, was developed. The OFF-ON switch of **HPL-1** can be triggered via pH-induced structural change of the lactam group of the rhodamine moiety from closed-ring to open-ring. Our results showed that the phosphate group of **HPL-1** is beneficial to its accumulation in liver cells, and combination of the phosphate and galactose units could synergistically increase the hepatocyte-targeting capacity. **HPL-1** could selectively distinguish hepatoma cells from other tissue cells, and precisely distinguish cancerous liver cells from normal liver cells. Compared with other reported probes, **HPL-1** not only enable a simple and convenient detection method, but also has good hepatocyte-targeting capacity and precise recognition capacity of tumors under weak acid micro-environment, which opens new avenues for precise diagnosis and treatment of hepatocellular carcinoma.

Keywords: hepatocyte-targeting; fluorescent probe; tumorous pH; phosphate; galactose

---

1. Introduction

Hepatocellular carcinoma (HCC) is one of the most dangerous malignancies associated with high incidence and low survival rate[1, 2]. HCC is often diagnosed at the advanced stage[3], when the surgical removal is not applicable any more. Therefore, considerable efforts have been devoted to the early and accurate detection of HCC, and a series of biomarkers have been developed for the specific recognition of HCC[4]. However, while these methods could partially identify cancer cells, they suffer from some drawbacks such as the complex pretreatment, high cost, time-consuming, or difficult for storing.

It has been well-known that the pH value of tumorous micro-environment (6.2~6.9)[5,6] is slightly lower than that of physiological micro-environment (7.2~7.4)[7]and this phenomenon has arisen from the unlimited propagation of cancer cells in the oxygen-deficient environment. Therefore, precise differentiation of the subtle pH value change would provide an ideal and practical approach to distinguish cancerous cells from normal cells. Rhodamines[8-11], naphthalimides[12,13], benzoindole[14-16], and a series of nanomaterials[17] are well-established pH-responsive probes with good optical performance, spatial-temporal feature, high sensitivity and selectivity[18]. However, they are mainly used to monitor pH changes under acidic conditions (pH < 5.5). Currently, there are no a small molecule probes able to accurately differentiate pH values of cancer cells from normal cells.

It has been well-documented that galactose can be recognized by asialoglycoprotein receptor (ASGPR) overexpressed on the hepatocytes[19-24]. On the other hand, organic molecules bearing a phosphate or phosphoric acid group such as Sofosbuvir and Adefovir were found to easily accumulate in liver (ProTide technology)[25,26]. However, the hepatocyte-targeting capacity of either galactose or phosphate is still unsatisfactory. In our efforts to develop a simple, efficient, and accurate method to distinguish cancerous liver cells from normal liver cells, galactose and phosphate have been integrated in this study as a dual hepatocyte-targeting motif with the rhodamine derivative as a pH-responsive fluorophore. On the basis of this, a novel small molecule dual hepatocyte-targeting probe (**HPL-1**) for specific detection of HCC has been developed for the first time (**Fig. 1**).

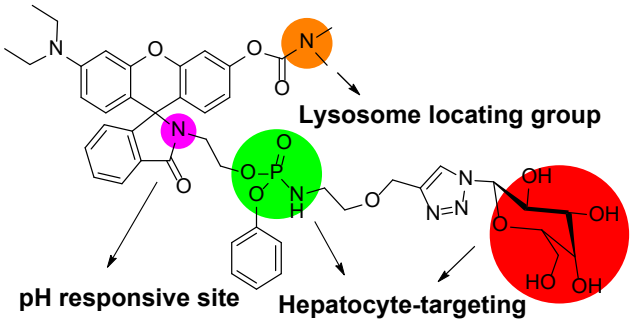

Fig. 1. Structure of HPL-1

2. Experimental Section

2.1. Materials and Instruments.

All reactants were commercially purchased without further purification. Phenyl dichlorophosphate is purchased from Damas-beta (China). 2-(4-Diethylamino)-2-hydroxybenzoyl) benzoic acid and Dimethylcarbamoyl chloride was purchased from Jiuding Chemical (Shanghai, China). β-Galactose were obtained from Xilong Chemical (Guangdong, China). Resorcinol is acquired from Damao Chemical (Tianjin, China). Ethanolamine is supplied by Sinopharm Group Chemicals (Shanghai, China).^{1}H NMR and ^{13}C NMR spectra were recorded on a Bruker 600 MHz (Switzerland) at 25 °C, with TMS as the internal standard in CDCl3, and the solvent peak as the internal reference in CD3OD. MS analysis was performed with a Thermo Fisher Scientific LTQ FT Ultra (USA). The UV-vis absorption and fluorescence spectra were obtained with a Shanghai JingHua 7600 UV-visible spectrophotometer (dual beam) (China) and a Shimadzu RF-5301PC (Japan) at room temperature, respectively. The cytotoxicity assays were conducted using ELX800 absorbance microplate reader. Cell image assays were performed by Multi-photon laser confocal scanning microscopy (a LEICA-TCS-SP8MP) (Germany).

2.2. Synthesis of HPL-1.

Synthesis of **HPL-1** commenced with the cyclization of 2-(4-diethylamino)-2-hydroxybenzoyl)benzoic acid and resorcinol under acidic conditions to give a rhodamine derivatives **1**[27]. Esterification of this compound with dimethylcarbamoyl chloride afforded the carbamate compound **2**. Treatment of compound **2** with ethanolamine provided the amide compound **3** which was subsequently converted to the phosphate compound **6** with phenyl dichlorophosphate followed by the primary amine **5**. Then, the alkyne compound **6** underwent a click reaction to generate the triazole compound **8** which provided the desired molecule **HPL-1** upon saponification (**Scheme 1**). The structures of all compounds were characterized by ^{1}H NMR, ^{13}C NMR, and MS spectrometry (Supplementary Information).

Scheme 1. The synthesis of HPL-1.

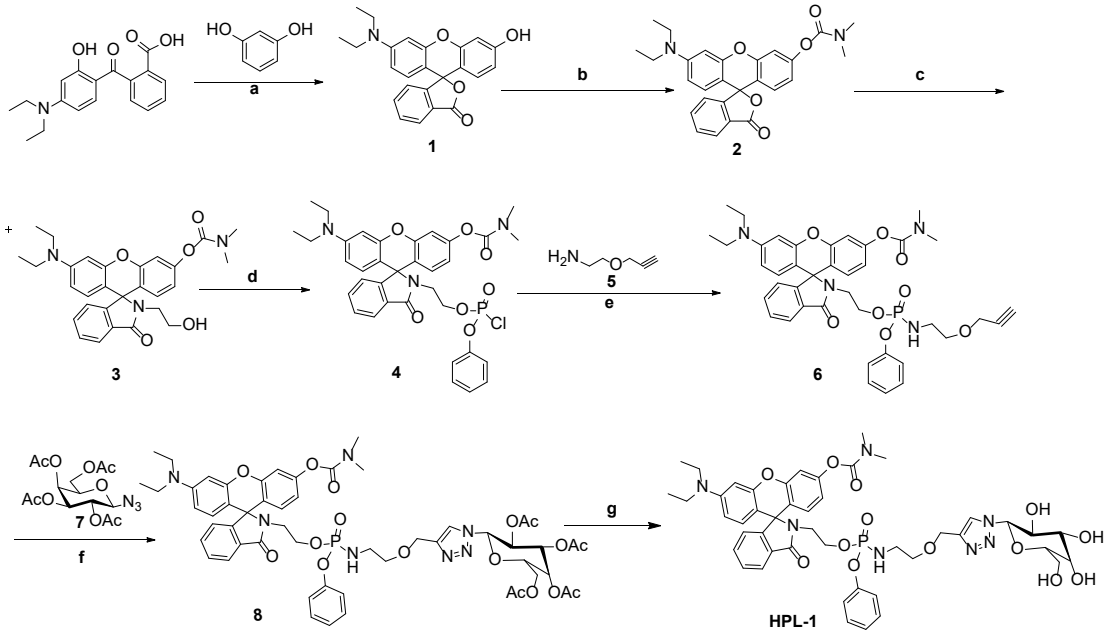

(a) CF_3COOH, 90°C, Reflux for 24h, (95%) (b) Dimethylcarbamoyl chloride, KOH, DMF (50%) (c) Ethanolamine, C_2H_5OH, 90°C, Reflux (43%) (d) Phenyl dichlorophosphate, Et_3N, DCM, -40 °C (e) Compound 5, Et_3N, DCM, -40 °C (58%) (f) Compound 7, NaVc, $CuSO_4.5H_2O$, THF: H_2O (v:v=1:1), (89%) (g) CH_3ONa, CH_3OH (95%).

2.3. Spectral testing

The probe HPL-1 was dissolved in DMSO to prepare a 1 mM stock solution. Take 100 μL stock solution in a 5 mL centrifuge tube, then set the volume to 5 mL with different pH buffer solution to form 20 μM HPL-1 solution. The test solution is poured into the cuvette. UV spectral scanning range is 200 nm-800 nm. Fluorescence spectrum scanning range is 300 nm-700 nm. Slit width is 3 nm×3 nm.

2.4. Cell culture and Confocal Microscopy Imaging

HepG2 cells were incubated with 20 μM HPL-1 for 30 min at 37°C. Then, the cells were washed with PBS for three times and fixed with 4% paraformaldehyde for 15 min at room temperature. After washing with PBS for three times, the cells were soaked in buffer solution (pH 6.5) and buffer solution (pH 7.4) for 10 min, respectively.

HepG2 cells were incubated with 20 μM HPL-1 for 30 min at 37°C. Then, the cells were washed with PBS for three times and fixed with 4% paraformaldehyde for 15 min. After washing with PBS for three times, HepG2 cells were soaked in buffer solution (pH 6.5) for 10 min, and L02 cells were soaked in buffer solution (pH 7.4) for 10 min.

HepG2, A549, SGC-7901 and Hela cells were treated with 20 μM HPL-1 for 30 min at 37°C. Subsequently, the cells were washed with PBS for three times and fixed with 4% paraformaldehyde for 15 min. After washing with PBS for three times, the cells were soaked in buffer solution (pH 6.5) for 10 min.

HepG2 cells were incubated with 20 μM Compound 3 (without phosphate group and gatactose group), Compound 6 (with phosphate group) and HPL-1 (with phosphate and gatactose groups) for 30 min at 37°C, respectively. Subsequently, the cells were washed with PBS for three times and fixed with 4% paraformaldehyde for 15 min. After washing with PBS for three times, the cells were treated by buffer solution (pH 6.5) for 10 min.

To illuminate localization of HPL-1 in lysosome**,** HepG2 cells were seeded in glass bottom dish to incubate for 24 h at 37 °C under 5% CO2. Then, the cells were incubated with LysoTracker (500 nM) for 30 min. Next, the cells were washed by PBS for three times and treated by HPL-1 (20 μM) for another 30 min. Finally, the cells were washed thrice with PBS.

All fluorescence images were collected with Multi-photon laser confocal scanning microscopy (Germany). Probes were excited at 488 nm and their green emissions were collected in the range of 490−530 nm. More experimental details were shown in the results and discussion.

2.5 Cytotoxicity assays.

HepG2 cells were seeded in 96-well plates with a density of 6000 cells per well and incubated for 24 h at 37 °C under 5% CO2. Then, the cells were treated with the different concentrations of HPL-1 (0-20 μM) for 48 h. Subsequently, 10 μL MTT (5 mg/ml) was added to incubate for 4 h. After that, the medium was replaced by 150 μL DMSO. After gentle shaking for 10 min, and the OD values were recorded by an ELX800 absorbance plate reader (USA) at 490 nm.

3. Results and Discussion

3.1. Spectral Properties of HPL-1 at Different pH Values

To explore the sensitivity of **HPL-1** toward the pH values, the fluorescence titration experiments were carried out (**Fig. 2**). It was noticed that the fluorescence spectra of **HPL-1** solution shows two distinct peaks at pH 6.5 and pH 7.4. Additionally, the fluorescence intensity of this compound at pH 6.5 is obviously stronger than that at pH 7.4. Presumably, **HPL-1** adopts a non-conjugated closed-ring lactam conformation at pH 7.4 with weak fluorescence from the rhodamine moiety. Once the pH value is decreased to 6.5, the lactam ring of **HPL-1** could be opened to give an extended conjugated system with strong fluorescent[28, 29]. Clearly, **HPL-1** is a highly pH-sensitive probe in the narrow range of pH 6.0~7.5, and is capable of monitoring the pH change in weak acidic environment. Thus, **HPL-1** has the potential to distinguish cancer cells with the pH value of 6.2~6.9 from normal cells (pH 7.2~7.4). To illuminate the effect of phosphate group of **HPL-1** on the sensitivity toward the pH values, the fluorescence

properties of **Compound 3** without phosphate group toward the pH value were comparatively analyzed (**Fig. S1**). From **Fig. S1** and **Fig. 2**, **HPL-1** and **Compound 3** present similar fluorescence tendency, but **HPL-1** shows stronger fluorescence intensity than **Compound 3**, suggesting that the introduction of phosphate group does not modify detection range of pH values (6.0~7.5), but it is beneficial for the sensitivity toward the pH value.

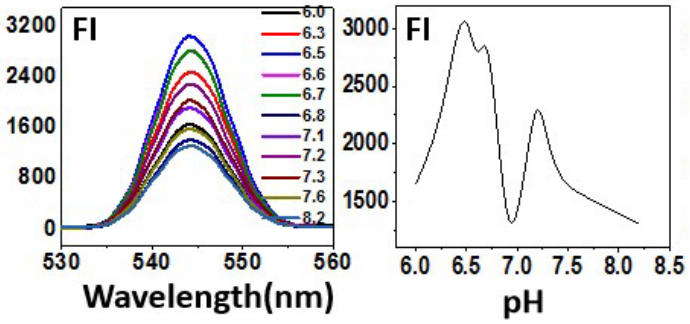

Fig. 2. Fluorescence intensity (FI) of **HPL-1** (20 μM) at different pH values in Britton−Robinson (BR) buffer solution. λ_{ex} = 273 nm, λ_{em} = 544nm. Slit width: 3nm×3 nm.

3.2. Cellular pH sensitivity of HPL-1 at pH 6.5 and 7.4

To further explore whether **HPL-1** can accurately distinguish weak acid environment of cancer cells from weak basic environment of normal cells, cell imaging experiments of **HPL-1** at pH 6.5 and 7.4 were performed. As shown in **Fig. 3**, the fluorescence intensity of **HPL-1** in the cells with medium pH of 6.5 was about 4 times that of **HPL-1** in the cells with medium pH of 7.4, being consistent with the fluorescence spectra *in vitro*. This result suggests that **HPL-1** can be used to accurately distinguish cancer cell micro-environment (pH 6.5) from normal cell micro-environment (pH 7.4).

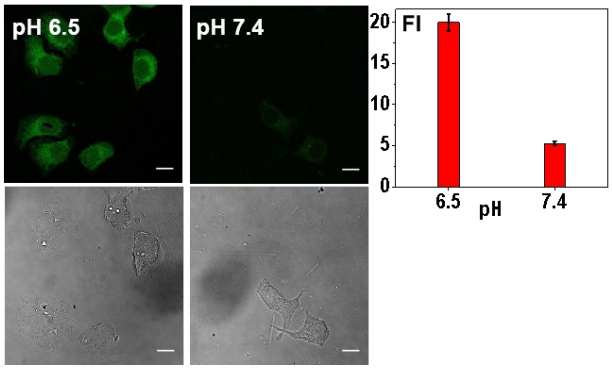

Fig. 3. Fluorescence imaging of **HPL-1** (20 μM) in HepG2 cells treated with pH 6.5 and pH 7.4 Britton−Robinson (BR) buffer solutions for 30 min, respectively. Scale bar: 10 μm.

3.3. Cell imaging of HPL-1 in normal liver cells (L02) and hepatocellular carcinoma cells (HepG2 cell)

Next, we conducted a comparative cell imaging experiment of **HPL-1** in normal liver cells (L02) and cancerous liver cells (HepG2**)** to identify whether **HPL-1** can accurately

distinguish cancerous liver cells from normal liver cells. As shown in **Fig. 4**, the fluorescence intensity of **HPL-1** in HepG2 cells was about 6 times that of **HPL-1** in normal liver cells (L02), implying that **HPL-1** can be used to accurately distinguish cancerous liver cells from normal liver cells. When **Fig. 3** and **Fig. 4** are compared, the relative fluorescence intensity of HepG2 cells at pH 7.4 (~5) is stronger than that of L02 cells at pH 7.4 (~3), showing that HepG2 cells with high expression of ASGPR are more favourable for the endocytosis of **HPL-1** with a galactose group while L02 cells with low expression of ASGPR uptake less **HPL-1**. This is suggested that the expression of ASGPR is one influencing factor to cause the different uptake amount of **HPL-1**, resulting in the fluorescence difference of **HPL-1**. On the other hand, the relative fluorescence intensity of HepG2 cells at pH 6.5 (~20) is much stronger than that of HepG2 cells at pH 7.4 (~5), suggesting that the different pH value is the more important influencing factor to cause the fluorescence difference of **HPL-1**. This may be because **HPL-1** adopts a non-conjugated closed-ring lactam conformation with weak fluorescence at pH 7.4, and adopts an extended conjugated system with strong fluorescence at pH 6.5. On the whole, the significant difference of fluorescence intensity between HepG2 cells and L02 cells is simultaneously caused by the different expressions of ASGPR and the different pH values.

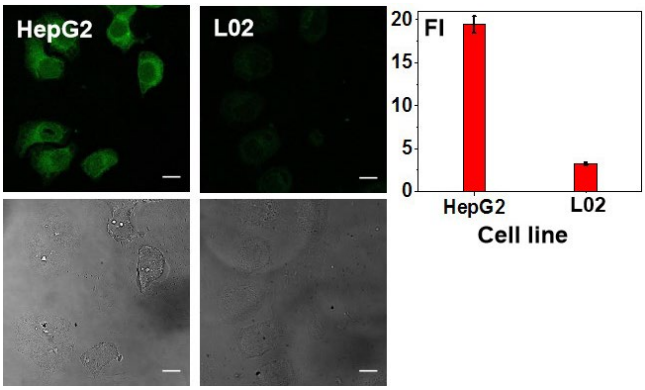

Fig. 4. Fluorescence imaging of **HPL-1** (20 μM) in HepG2 cells (medium pH 6.5) and L02 cells (medium pH 7.4). FI: Fluorescence intensity, Scale bar: 10 μm.

3.4. Cell imaging of HPL-1 in hepatocellular carcinoma cells (HepG2 cell) and other tissue cells

We then performed hepatocyte-targeting cell imaging experiments to exploit whether **HPL-1** is able to selectively distinguish hepatocellular carcinoma cells from other tissue cells (**Fig. 5**). It was found that although all of these cells showed green fluorescence, the fluorescence intensity of the HepG2 cell was about 6 times that of A549 cell, 15 times that of SGC-7901, and 12 times that of HeLa. These results suggest that **HPL-1** has good hepatocyte-targeting and could selectively distinguish

hepatocellular carcinoma cells from other tissue cells. The reason can be attributed to a fact that HepG2 cells with high expression of ASGPR possesses stronger phagocytosis capacity toward **HPL-1** with a galactose group than A549, SGC-7901 and Hela cells with low expression of ASGPR, thus causing the fluorescence difference of Cells. The difference in fluorescence intensity between A549, SGC-7901 and Hela cells can be also attributed to their difference of expression amounts of ASGPR under the same pH value.

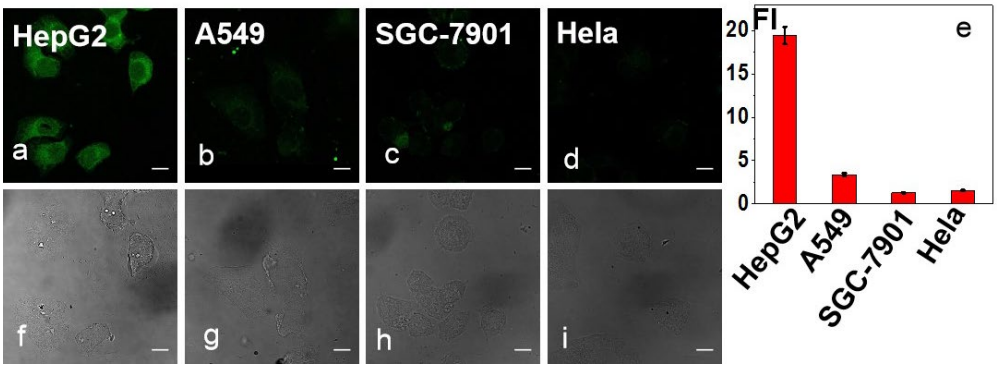

Fig. 5. Fluorescence imaging of **HPL-1** (20 μM) in HepG2, A549, SGC-7901 and HeLa cells treated with pH 6.5 BR buffer solutions for 30 min. FI: Fluorescence intensity, Scale bar: 10 μm.

3.5. The contribution of the HPL-1 fragment on liver-targeting capacity

To probe the role of key fragments of **HPL-1** on hepatocyte-targeting capacity, two representative **compounds 3** without phosphate group and gatactose group, **Compound 6** with phosphate group were prepared comparatively analyzed. As shown in **Fig. 6**, the fluorescence intensity of Compound **6** was stronger than that of compound **3**, indicating that the phosphate modification is beneficial for the hepatocyte-targeting strategy. The fluorescence intensity of **HPL-1** is significantly stronger than that of compound **6**, suggesting that the introduction of galactose group is favourable for hepatocyte-targeting capacity, which is attributed to the specific recognization of the galactose unit of **HPL-1** on ASGPR overexpressed on the hepatocytes. Furthermore, **HPL-1** exhibited much higher fluorescence intensity than **Compound 3** and **Compound 6**，showing that the co-modification with phosphate and galactose groups could synergistically improve hepatocyte-targeting effect of compounds, which is attributed to the superposition effect of phosphate and galactose.

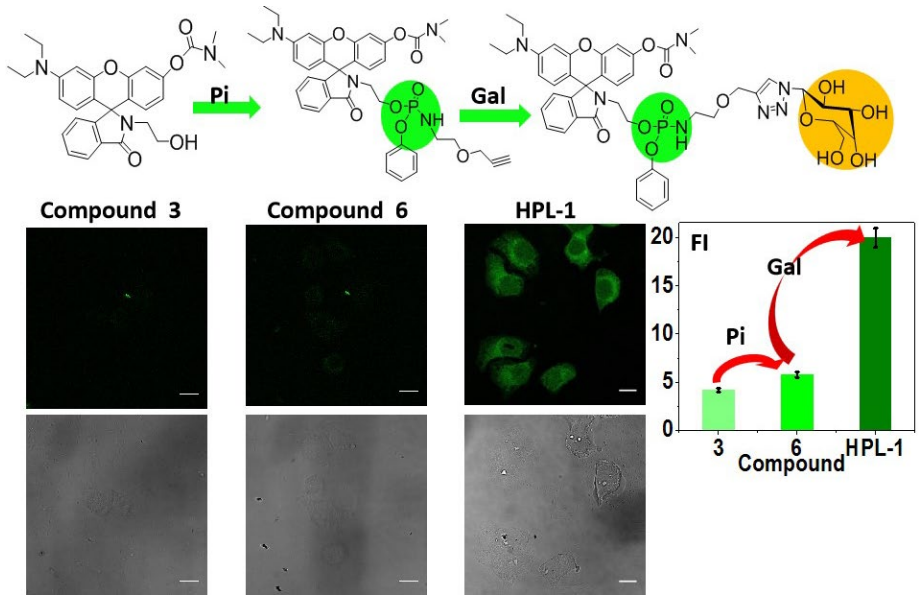

Fig.6. Fluorescence imaging of **Compound 3**, **Compound 6** and **HPL-1 (**20 μM**)** in HepG2 cells treated with pH 6.5 BR buffer solutions for 30 min. FI: Fluorescence intensity, Scale bar: 10 μm.

3.6. Galactose inhibition test

To further illuminate the contribution of galactose on the hepatocyte-targeting capacity of **HPL-1**, we performed galactose competition experiments. As shown in **Fig. 7**, the fluorescence intensity of **HPL-1** gradually decreased with the addition of galactose (0-40 μM), and the fluorescence can hardly be observed when galactose reached 40 μM. These results demonstrate that the specific recognition of galactose group on ASGPR is one of driving forces for the hepatocyte-targeting capacity of **HPL-1**.

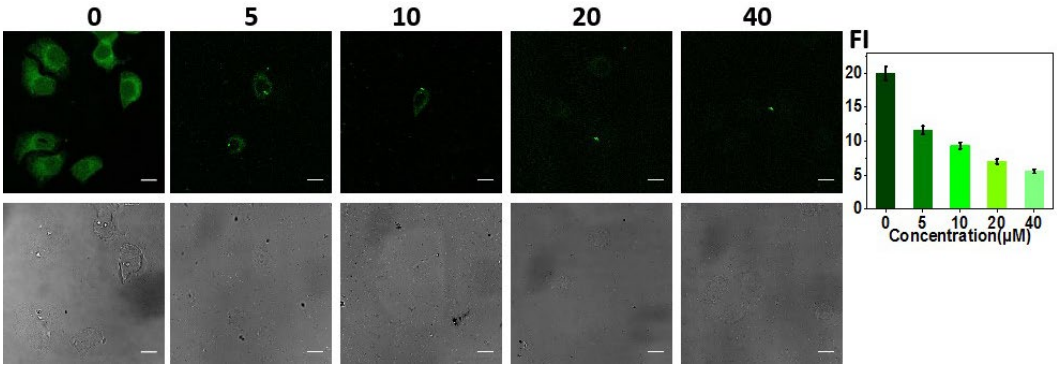

Fig. 7. Fluorescence imaging of **HPL-1** in HepG2 cells pretreated with different doses of galactose. Scale bar: 10 μm. FI: Fluorescence intensity.

Lysosome has been reported as an acid production center (pH 3.8-5.0) in living cells and may be directly related to an acidic micro-environment of cancer cells[30]. Therefore, it is very significant to illuminate whether **HPL-1** can reach intracellular lysosome. In

Fig. 8, the cells showed the pseudo-green fluorescence of **HPL-1** and the pseudo-red fluorescence of LysoTracker respectively. Furthermore, **HPL-1** and LysoTracker were well merged in HepG2 cells with the Mander's overlap coefficient of 0.94, suggesting that **HPL-1** could specifically reach intracellular lysosomes, which may be attributed to the attraction of the lysosomal acidic micro-environment to the alkaline dimethylamino group of **HLP-1.**

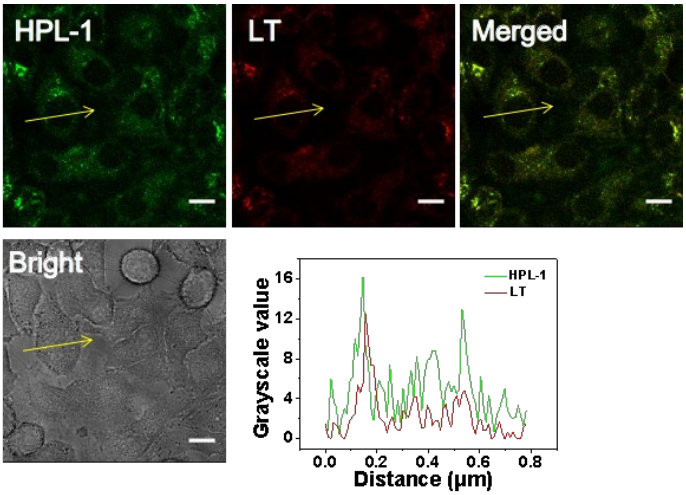

Fig. 8. Fluorescence imaging of HepG2 cells treated with 500 nM of LysoTracker **(LT)** and 20 μM of **HPL-1**. Merged image is the overlap of **HPL-1** and **LT**. The fluorescence intensity correlation plots of LT and HPL-1 (grayscale value).

3.7. Cytotoxicity

Low toxicity is an important requirement for fluorescent probes used in biological systems. As shown in **Fig. 9**, after HepG2 cells were incubated with **HPL-1** (<10 μM) for 24 hours, the cell viability was nearly 100%. Even when the concentration of **HPL-1** was increased to 20 μM, the cell viability was still above 80%. Clearly, **HPL-1** could be harmlessly used to detect hepatoma cells in biological system. The possible reason is that **HPL-1** contains biocompatible phosphate and galactose groups.

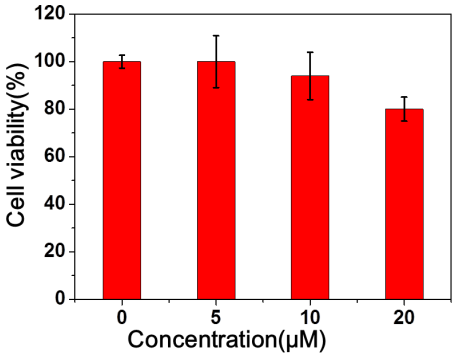

Fig. 9. Cell viability of HepG2 incubated with different concentrations of **HPL-1**.

The above results showed that compared with other pH fluorescent probes (**Table**

S1), **HPL-1** possesses the most narrow detection range of pH (6.4-6.7), which corresponds to the pH range of cancer micro-environment. Moreover, **HPL-1** showed excellent hepatocyte-targeting capacity (particularly for hepatoma cells).

4. Conclusion

A new dual hepatocyte-targeting fluorescent probe (**HPL-1**) has been developed in this study. This molecule switches on at tumorous micro-environment (pH 6.5), but switches off at physiological micro-environment (pH 7.4). **HPL-1** can distinguish hepatoma cells from other tissue cells, and it represents the first example of small molecules for specific hepatoma cell targeting. The observed hepatocyte-targeting capacity trend with compounds **3**, **6** and **HPL-1** indicates that while phosphate modification is an efficient hepatocyte-targeting strategy, and co-modification with phosphate and the galactose unit could synergistically improve hepatocyte-targeting effect of compounds. More importantly, **HPL-1** can precisely distinguish cancerous liver cells from normal liver cells via accurate response to adjacent tumorous and physiological pH. Moreover, the observed low-toxicity and ready availability of HPL-1 are beneficial to the detection of hepatoma cells *in vitro*, and is of great significance for the early diagnosis and precise treatment of hepatocellular carcinoma.

ASSOCIATED CONTENT

Supplementary data

The experimental details and compound characterizations. These materials are available free of charge via the Internet at https://doi.org.

AUTHOR INFORMATION

Corresponding Author

jianyiwang@gxu.edu.cn (W. J.); mianwang@gxu.edu.cn (W. M.)

Notes

The authors declare no competing financial interest.

ACKNOWLEDGMENT

This work was financially supported by Guangxi Key Laboratory of Traditional Chinese Medicine Quality Standards (201602), the Scientific Research Fund of

Guangxi Education Department (2018KY0044) and the Scientific Research Fund of Guangxi University (XJZ170410).

References

[1] S. K. Misra, G. Ghoshal, M. R. Gartia, Z. Wu, A. K. De, M. Ye, C. R. Bromfield, E. M. Williams, K. Singh, K. V. Tangella, L. Rund, K. Schulten, L. B. Schook, P. S. Ray, E. C. Burdette, D. Pan, Trimodal Therapy: Combining Hyperthermia with Repurposed Bexarotene and Ultrasound for Treating Liver Cancer, *Acs Nano.* 9(2015) 10695-10718.

[2] J. M. Ludwig, M. Xing, Y. K. Gai, L. Y. Sun, D. X. Zeng, H. S. Kim, Targeted Yttrium 89-Doxorubicin Drug-Eluting Bead A Safety and Feasibility Pilot Study in a Rabbit Liver Cancer Model, *Mol. Pharm*. 14(2017) 2824-2830.

[3] M. Fang, R. Adhikari, J. Bi, W. Mazi, N. Dorh, J. Wang, N. Conner, J. Ainsley, T. G. Karabencheva-Christova, F-T. Luo, A. Tiwari. H. Liu, Fluorescent probes for sensitive and selective detection of pH changes in live cells in visible and near-infrared channels, *J. Mater. Chem. B*. 5(2017) 9579-9590.

[4] D. Shangguan, L. Meng, Z. C. Cao, Z. Xiao, X. Fang, Y. Li, D. Cardona, R. P. Witek, C. Liu, W. Tan, Identification of Liver Cancer-Specific Aptamers Using Whole Live Cells, *Anal. Chem*. 80(2008) 721-728.

[5] G. Ke, Z. Zhu, W. Wang, Y. Zou, Z. Guan, S. Jia, H. Zhang, X. Wu, C. J. Yang, A Cell-Surface-Anchored Ratiometric Fluorescent Probe for Extracellular pH Sensing, *Appl. Mater. Inter.* 6(2014) 15329-15334.

[6] H-S. Lv, J. Liu, J. Zhao, B-X. Zhao, J-Y. Miao, Highly selective and sensitive pH-responsive fluorescent probe in living Hela and HUVEC cells, *Sensors and Actuat A-phys. B.* 177(2013) 956-963.

[7] M. Stubbs, P. M. J. McSheehy, J. R. Griffths, C. L. Bashford, Causes and consequences of tumour acidity and implications for treatment, *Elsevier Science Ltd*. 99(2000) 01615-01619.

[8] K. Zhou, H. Liu, S. Zhang, X. Huang, Y. Wang, G. Huang, B. D. Sumer, J. Gao, Multicolored pH-Tunable and Activatable Fluorescence Nanoplatform Responsive to Physiologic pH Stimuli, *J. Am. Chem. Soc.* 134(2012) 7803-7811.

[9] G. Niu, P. Zhang, W. Liu, M. Wang, H. Zhang, J. Wu, L. Zhang, P. Wang, Near-Infrared Probe Based on Rhodamine Derivative for Highly Sensitive and Selective Lysosomal pH Tracking, *Anal. Chem.* 89(2017) 1922-1929.

[10] M-C. Xia, L. Cai, S. Zhang, X. Zhang, Cell-Penetrating Peptide Spirolactam Derivative as a Reversible Fluorescent pH Probe for Live Cell Imaging, *Anal. Chem.* 89(2017) 1238-1243.

[11] U. Reddy G, A. H. A, F. Ali, N. Taye, S. Chattopadhyay, A. Das, FRET-Based Probe for Monitoring pH Changes in Lipid-Dense Region of Hct116 Cells, *Org. Lett.* 17(2015) 5532-5535.

[12] M. H. Lee, N. Park, C. Yi, J. H. Han, J. H. Hong, K. P. Kim, D. H. Kang, J. L.

Sessler, C. Kang, J. S. Kim, Mitochondria-Immobilized pH-Sensitive Off.On Fluorescent Probe, *J. Am. Chem. Soc.* 136(2014) 14136-14142.
[13] M. H. Lee, J. H. Han, P-S. Kwon, S. Bhuniya, J. Y. Kim, J. L. Sessler, C. Kang, S. J. Kim, Hepatocyte-Targeting Single Galactose-Appended Naphthalimide: A Tool for Intracellular Thiol Imaging in Vivo, *J. Am. Chem. Soc.* 134(2012) 1316-1322.
[14] W. Niu, L. Fan, M. Nan, Z. Li, D. Lu, M. S. Wong, S. Shuang, C. Dong, Ratiometric Emission Fluorescent pH Probe for Imaging of Living Cells in Extreme Acidity, *Anal. Chem.* 87(2015) 2788-2793.
[15] X. Zhang, N. He, Y. Huang, F. Yu, B. Li, C. Lv, L. Chen, Mitochondria-targeting near-infrared ratiometric fluorescent probe for selective imaging of cysteine in orthotopic lung cancer mice, *Sensor Actuat B-chem*. 282(2019) 69-77.
[16] M. Gao, F. Yu, C. Lv, J. Ghoo, L. Chen, Fluorescent chemical probes for accurate tumor diagnosis and targeting therapy, *Chem. Soc. Rev.* 46(2017) 2237-2271.
[17] Z-Y. Qiao, C-Y. Hou, W-J. Zhao, D. Zhang, P-P. Yang,; L. Wang,; H. Wang, Synthesis of self-reporting polymeric nanoparticles for in situ monitoring of endocytic microenvironmental pH, *Chem. Commun.* 51(2015) 12609-12612.
[18] M. H. Lee, E-J. Kim, H. Lee, H. M. Kim, M. J. Chang, S. Y. Park, K. S. Hong, J. S. Kim, J. L. Sessler, Liposomal Texaphyrin Theranostics for Metastatic Liver Cancer, *J. Am. Chem. Soc.* 138(2016) 16380-16387.
[19] J. An, X. Dai, Z. Wu, Y. Zhao, Z. Lu, Q. Guo, X. Zhang, G. Li, An Acid-Triggered Degradable and Fluorescent Nanoscale Drug Delivery System with Enhanced Cytotoxicity to Cancer Cells, *Biomacromolecules.* 16(2015) 2444-2454.
[20] L. Fu, C. Sun, L. Yan, Galactose Targeted pH-Responsive Copolymer Conjugated with Near Infrared Fluorescence Probe for Imaging of Intelligent Drug Delivery, *ACS Appl. Mater. Inter.* 7(2015) 2104-2115.
[21] C. Duan, J. Gao, D. Zhang, L. Jia, Y. Liu, D. Zheng, G. Liu, X. Tian, F. Wang, Q. Zhang, Galactose-Decorated pH-Responsive Nanogels for Hepatoma-Targeted Delivery of Oridonin, *Biomacromolecules.* 12(2011) 4335-4343.
[22] S. Quan, Y. Wang, A. Zhou, P. Kumar, R. Narain, Galactose-based Thermosensitive Nanogels for Targeted Drug Delivery of Iodoazomycin Arabinofuranoside (IAZA) for Theranostic Management of Hypoxic Hepatocellular Carcinoma, *Biomacromolecules.* 16(2015) 1978-1986.
[23] B. Thapa, P. Kumar, H. Zeng, R. Narain, Asialoglycoprotein Receptor-Mediated Gene Delivery to Hepatocytes Using Galactosylated Polymers, *Biomacromolecules.* 16(2015) 3008-3020.
[24] C-H. Lai, T-C. Chang, Y-J. Chuang, D-L. Tzou, C-C. Lin, Stepwise Orthogonal Click Chemistry toward Fabrication of Paclitaxel/Galactose Functionalized Fluorescent Nanoparticles for HepG2 Cell Targeting and Delivery, *Bioconjugate Chem.* 24(2013) 1698-1709.
[25] Y. Mehellou, H. S. Rattan, J. Balzarini, The ProTide Prodrug Technology: From the Concept to the Clinic Miniperspective, *J. Med. Chem.* 61(2018) 2211-2226
[26] F. Pertusati, C. McGuigan, Diastereoselective synthesis of P-chirogenic phosphoramidate prodrugs of nucleoside Analogues (ProTides) via copper

catalysed reaction, *Chem. Commun.* 51(2015) 8070-8073.
[27] H. Li, C. Wang, M. She, Y. Zhu, J. Zhang, Z. Yang, P. Liu, Y. Wang, J. Li, Two rhodamine lactam modulated lysosome-targetable fluorescence probes for sensitively and selective monitoring subcellular organelle pH change, *Spectrochim Actaa*. 900(2015) 97-102.
[28] K. Tiensomjitr, R. Noorat, K. Wechakorn, S. Prabpai, K. Suksen, P. Kanjanasirirat, Y. Pewkliang, S. Borwornpinyo, P. Kongsaeree, A rhodol-based fluorescent chemosensor for hydrazine and its application in live cell bioimaging, *Mol. Biomolecular Spectroscopy*. 185(2017) 228-233.
[29] W. Niu, M. Nan, L. Fan, W. S. Wong, S. Shuang, C. Dong, A novel pH fluorescent probe based on indocyanine for imaging of living cells, *Dyes Pigments.* 126(2016) 224-231.
[30] W. Ma, L. Yan, X. He, T. Qing, Y. Lei, Z. Qiao, D. He, K. Huang, K. Wang, Hairpin-Contained i-Motif Based Fluorescent Ratiometric Probe for High-Resolution and Sensitive Response of Small pH Variations, *Anal. Chem.* 90(2018) 1889-1896.